The Astrophysical Journal, 649: L17–L20, 2006 September 20

DETECTION OF C_3O IN IRC +10216: OXYGEN-CARBON CHAIN CHEMISTRY IN THE OUTER ENVELOPE

E. D. Tenenbaum, A. J. Apponi, and L. M. Ziurys
Departments of Chemistry and Astronomy, Arizona Radio Observatory, Steward Observatory, University of Arizona, 933 North Cherry Avenue, Tucson, AZ 85721; emilyt@as.arizona.edu, aapponi@as.arizona.edu, lziurys@as.arizona.edu
M. Agúndez, J. Cernicharo, and J. R. Pardo
Departamento de Astrofísica Molecular e Infrarroja, Instituto de Estructura de la Materia, CSIC, Serrano 121, E-28006 Madrid, Spain; marce@damir.iem.csic.es, cerni@damir.iem.csic.es, pardo@damir.csic.es
and
M. Guélin
Institut de Radioastronomie Millimétrique, 300 rue de la Piscine, F-38406 St. Martin d'Héres, France guelin@iram.fr
Received 2006 June 28; accepted 2006 August 3; published 2006 September 8

ABSTRACT

The oxygen-bearing species C_3O has been identified in the circumstellar envelope of the carbon star IRC +10216. The $J = 8 \rightarrow 7$, $9 \rightarrow 8$, $10 \rightarrow 9$, $14 \rightarrow 13$, and $15 \rightarrow 14$ transitions were detected at 2 and 3 mm using the Arizona Radio Observatory's 12 m telescope. Measurements of the $J = 9 \rightarrow 8$, $10 \rightarrow 9$, and $12 \rightarrow 11$ lines were simultaneously conducted at the IRAM 30 m telescope. The line profiles of C_3O are roughly U-shaped, indicating an extended shell distribution for this molecule in IRC +10216. The total column density derived for C_3O is 1.2×10^{12} cm^{-2}, at least an order of magnitude higher than that predicted by current chemical models. However, a revised model that includes reactions of atomic oxygen with carbon-chain radicals, such as l-C_3H and C_4, can reproduce the observed abundance. This model also predicts that C_3O arises from a shell source with an outer radius near $r \sim 30''$, consistent with the observations. These results suggest that gas phase neutral-neutral chemistry may be producing the oxygen-bearing molecules present in the outer envelope of IRC +10216.

Subject headings: astrochemistry — circumstellar matter — ISM: molecules — radio lines: stars — stars: carbon — stars: individual (IRC +10216)

1. INTRODUCTION

IRC +10216 is a low-mass asymptotic giant branch star that is losing its outer atmosphere at a rate of $(2–4) \times 10^{-5}$ $M_\odot$ yr^{-1}, creating a dusty, molecule-rich extended circumstellar envelope. The process of dredge-up that occurs at this evolutionary stage has altered the elemental composition at the surface of this star such that C > O, as opposed to the solar ratio of C < O (Savage & Sembach 1996). Because of this carbon enrichment, the bulk of oxygen in IRC +10216 is contained in the highly stable species, CO. Under the LTE conditions of the inner envelope, CO is a very effective reservoir for oxygen; consequently, the only other O-bearing species with a significant abundance is SiO (e.g., Morris et al. 1975). Furthermore, oxygen remains in the form of CO throughout the circumstellar shell. This molecule has in fact been observed to a radius of 140″ in IRC +10216 (Fong et al. 2003).

Recently, however, other oxygen-bearing molecules have been detected in the circumstellar shell of IRC +10216, including H_2O (Melnick et al. 2001; Hasegawa et al. 2006), OH (Ford et al. 2003), and H_2CO (Ford et al. 2004). The existence of these species has been attributed to the vaporization of cometary ices from Kuiper Belt–type objects orbiting this star, which during the red giant phase released water and produced a new source of oxygen (Melnick et al. 2001). An alternative explanation (Agúndez & Cernicharo 2006) is that O-bearing compounds are formed in the outer envelope via neutral-neutral reactions between atomic oxygen, created by the photodissociation of CO, and abundant hydrocarbon radicals (e.g., Cernicharo et al. 2000). Moreover, studies of oxygen-rich circumstellar shells have demonstrated that their chemistry is not entirely controlled by the C/O ratio. Carbon-bearing species have now been found in numerous O-rich envelopes. For example, HCN, CS, HNC, and CN have been identified in TX Cam (e.g., Bujarrabal et al. 1994) and CS, HCN, CN, and HCO^+ in VY CMa (Milam et al. 2006). Kuiper Belt–like objects cannot explain these results. If C-bearing compounds are common to oxygen-rich circumstellar shells, then the converse is also likely to be true, namely, that C-rich envelopes contain nonnegligible abundances of O-containing molecules.

Here we report the detection of a new oxygen-bearing molecule in IRC +10216, C_3O. This species has been identified in the circumstellar envelope of this star via six rotational transitions observed in the 2 and 3 mm bands, using both the ARO 12 m and the IRAM 30 m telescopes. The spectra obtained for this molecule from both telescopes exhibit U-shaped line profiles, suggesting that C_3O has an extended, outer shell distribution. The abundance derived for C_3O is ~10 times greater than that predicted by recent circumstellar ion-molecule type models but can be reproduced if certain neutral-neutral reactions are considered. In the following sections, we present our observations, analyze the C_3O abundance, and discuss its implications for circumstellar chemistry.

2. OBSERVATIONS

Observations were conducted at the Arizona Radio Observatory (ARO)[1] 12 m telescope located at Kitt Peak, Arizona and the 30 m IRAM telescope at Pico Veleta, Spain. Observing frequencies, beam efficiencies, and beam sizes are listed in Table 1.

The ARO 12 m observations were carried out in a series of runs from 2003 October to 2005 December. The receivers used

[1] The Arizona Radio Observatory (ARO) is operated by Steward Observatory, University of Arizona, with partial support from the Research Corporation.

TABLE 1
OBSERVATIONS OF C_3O TOWARD IRC +10216

Transition	ν (MHz)	Telescope	θ (arcsec)	η^a	T_R^{*b} (mK)	v_{LSR} (km s^{-1})	$\Delta v_{1/2}$ (km s^{-1})	$\int T_R^* dv$ (K km s^{-1})
$8 \rightarrow 7$	76972.6	ARO 12 m	82	0.93	6.4 ± 1.5	−26.4 ± 3.9	25.9 ± 3.9	0.13 ± 0.02
$9 \rightarrow 8$	86593.7	ARO 12 m	73	0.90	4.0 ± 1.5	−27.1 ± 3.5	27.9 ± 3.5	0.10 ± 0.02
$9 \rightarrow 8$	86593.7	IRAM 30 m	28	0.82	12.5 ± 2.0	−26.1 ± 3.5	27.7 ± 3.5	0.22 ± 0.03
$10 \rightarrow 9$	96214.6	ARO 12 m	65	0.88	5.5 ± 1.1	−24.2 ± 3.1	30.5 ± 3.1	0.12 ± 0.02
$10 \rightarrow 9$	96214.6	IRAM 30 m	26	0.80	12.1 ± 3.0	−27.6 ± 3.1	28.6 ± 3.1	0.17 ± 0.03
$12 \rightarrow 11$	115455.9	IRAM 30 m	21	0.78	13.0 ± 5.0	−28.1 ± 2.6	33.7 ± 2.6	0.30 ± 0.08
$14 \rightarrow 13$	134696.3	ARO 12 m	47	0.79	4.9 ± 1.4	−25.5 ± 2.2	24.8 ± 2.2	0.09 ± 0.02
$15 \rightarrow 14$	144316.1	ARO 12 m	44	0.76	4.0 ± 1.6	−25.8 ± 2.1	27.4 ± 2.1	0.07 ± 0.02

[a] Main beam efficiency depending on temperature scale (η_c for 12 m data, η_b/η_{fss} for IRAM 30 m; $\eta_{fss} = 0.95$ for the IRAM 30 m; see http://www.iram.fr).
[b] Assumes filling factor of 1.

were dual-channel, cooled SIS mixers at 2 and 3 mm, operated in single-sideband mode with ~18 dB rejection of the image sideband. The back ends used were two 256 channel filter banks with 1 and 2 MHz resolutions, configured in parallel mode (2 × 128 channels) for the two receiver channels. A millimeter autocorrelator spectrometer (MAC) with 2048 channels of 768 kHz resolution was operated simultaneously to confirm features seen in the filter banks. The temperature scale, given in terms of T_R^*, was determined by the chopper wheel method corrected for forward spillover losses. The parameter T_R is then defined as $T_R = T_R^*/\eta_c$, where η_c is the corrected beam efficiency. Data were taken in beam switching mode with a $\pm 2'$ subreflector throw. Local oscillator shifts were done for each line to minimize image contamination.

The IRAM 30 m observations were done in several sessions from 1990 to 2005, primarily after 2002 in the context of a 3 mm line survey project. Two 3 mm SIS receivers with orthogonal polarizations were used in single side band mode with image rejections >20 dB. The temperature scale is T_A^*, where $T_R = T_A^* (\eta_{fss}/\eta_b)$. The standard wobbler switching mode was used with an offset of 4′. The back end used was a filterbank with a bandwidth of 512 MHz and a resolution of 1 MHz. Pointing and focusing were carried out at both telescopes by observing planets. The position used for IRC +10216 was $\alpha = 9^h45^m14\overset{s}{.}8$, $\delta = 13°30'40''$ (1950.0).

3. RESULTS

Figure 1 displays the six transitions of C_3O detected toward IRC +10216 using the 12 m and 30 m telescopes. The $J = 10 \rightarrow 9$ and $J = 9 \rightarrow 8$ lines were observed with both telescopes (both spectra are shown), while the $J = 8 \rightarrow 7$, $J = 14 \rightarrow 13$, and $J = 15 \rightarrow 14$ transitions were measured only at the 12 m, and the $J = 12 \rightarrow 11$ line only at IRAM. The line profiles in all six of these spectra are somewhat U-shaped, although the "U" is most prominent in the $J = 9 \rightarrow 8$ line measured at the 30 m and the $J = 10 \rightarrow 9$ transition from the 12 m. There is also about a factor of 2 difference in the radiation temperature for the $J = 9 \rightarrow 8$ line in the IRAM versus ARO spectrum. These findings suggest that the source of C_3O emission is extended with respect to the IRAM beam (~30″) but not uniformly filling the 12 m beam at 3 mm (~70″). (The $J = 11 \rightarrow 10$ transition near 105.8 GHz was observed, but it was severely contaminated by the $J = 23/2 \rightarrow 21/2$, $^2\Pi_{3/2}$, $v_7 = 1$ line of C_4H.)

Table 1 lists the line parameters determined for the observed C_3O transitions. The integrated intensities were derived using a shell fit. As the table illustrates, the C_3O features have an LSR velocity near −26.0 km s^{-1} and line widths in the range ~25–31 km s^{-1}—typical line parameters for IRC +10216. The antenna temperatures among the spectra from the two telescopes are also consistent, with $T_R \sim 4$–7 mK for the 12 m lines and $T_R \sim 15$ mK for the IRAM data. The consistency of the line profiles is additional evidence that they all arise from the same molecule.

4. ANALYSIS AND DISCUSSION

4.1. *Abundance and Distribution*

Because the line profiles from the 12 m are roughly U-shaped, it is reasonable to assume as a first approximation that C_3O emission fills all telescope beams. Under this assumption, a rotational diagram has been constructed for C_3O from the 12 m data using the integrated line intensities. This diagram yields a beam-filled column density of $N_{tot}(C_3O) = (1.2 \pm 0.4) \times 10^{12}$ cm^{-2} and a rotational temperature T_{rot} of 27 ± 7 K, where the errors reflect the uncertainty in the fits to the line profiles.

We also performed nonlocal, non-LTE radiative transfer calculations using the Monte Carlo formalism. We have assumed a spherical expanding envelope with the radial profiles of density and kinetic temperature used in Agúndez & Cernicharo (2006). The coefficients for collisional excitation of C_3O are assumed to be those of HC_3N-He (Green & Chapman 1978) corrected for H_2 as a collision partner. A reasonable fit to the line profiles observed with both telescopes was generated assuming a shell distribution with an inner radius of ~2×10^{16} cm ($r \sim 9''$), an outer radius between 5×10^{16} and 10^{17} cm ($r \sim 22''$–$45''$), and a radial column density of $N_{rad}(C_3O) = 1.3 \times 10^{12}$ cm^{-2} (N_{tot} equals $2N_{rad}$).

From 3 mm observations conducted with the 30 m telescope (J. Cernicharo et al. 2006, in preparation), we have also derived 3 σ upper limits for the column densities of other C_nO species, assuming a rotational temperature of 30 K: $N_{tot}(C_2O) < 7 \times 10^{12}$ cm^{-2}, $N_{tot}(C_4O) < 6 \times 10^{12}$ cm^{-2}, and $N_{tot}(C_5O) < 3 \times 10^{12}$ cm^{-2}.

4.2. *Chemical Synthesis of* C_3O

To elucidate the chemical origin of C_3O in IRC +10216, we have extended the chemical model described in Agúndez & Cernicharo (2006) to include oxygen-carbon chains C_nO, as well as related species such as $H_mC_nO^+$. In Figure 2 we plot the resulting abundance radial profiles, as well as the C_3O chemical scheme with the main formation routes. C_3O is produced through the dissociative recombination of several molecular ions $H_mC_nO^+$, which in turn are formed via (1) ion-molecule reactions involving atomic oxygen and (2) radiative associations between CO and unsaturated hydrocarbon ions. The resulting peak abundance relative to H_2 is 10^{-10} with a corresponding column density of

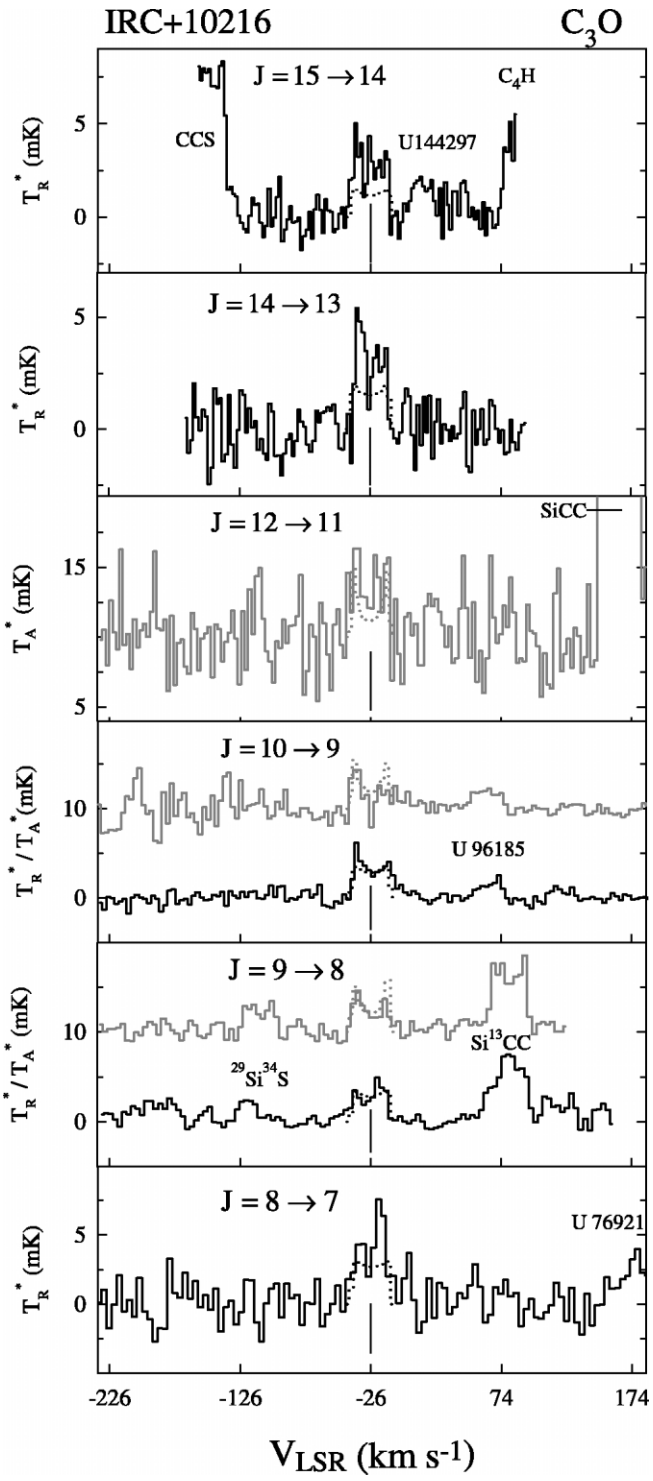

FIG. 1.—Spectra of the rotational transitions of C_3O observed toward IRC +10216 using the ARO 12 m (*solid black lines*) and IRAM 30 m (*solid gray lines*) telescopes. Dashed lines are the predictions of the radiative transfer model using the abundance profile $C_3O^{[O+C_4]}$ (see Fig. 2). The $C_3O^{[O+C_3H]}$ model essentially produces equivalent results. The temperature scales are T_R^* (12 m) and T_A^* (30 m). The IRAM data have been shifted upward by 10 mK and scaled by a factor of 0.4 for a better comparison. Filter resolution is 1 MHz.

$N_{rad}(C_3O) \sim 10^{11}$ cm^{-2}—roughly an order of magnitude lower than the value estimated from observations. Previous chemical models of IRC +10216 predict similar column densities for C_3O. For example, Millar et al. (2000) derive $N_{rad}(C_3O) = 3.4 \times 10^{10}$ cm^{-2}, a lower value because they do not include the $H_3C_3O^+$ species; in our model, this ion is one of the main intermediates in the synthesis of C_3O. The order-of-magnitude discrepancy between chemical models and the observations could be attributed to uncertainties in the rate constants. For example, the rates for the radiative associations between CO and the hydrocarbon ions are extrapolated from the analogous three-body associations with an estimated uncertainty of an order of magnitude (Herbst et al. 1984).

Important reactions may be missing from the model that could also enhance the C_3O formation rate. Particularly, neutral-neutral reactions involving atomic oxygen and hydrocarbon radicals could be rapid enough at low temperatures, with the formation of oxygen-carbon chains as a viable channel. Whereas atomic carbon is known to react rapidly with unsaturated hydrocarbons at low temperatures (Smith et al. 2004 and references therein), little information exists on the analogous reactions with atomic oxygen. Smith et al. (2004) have assumed that the reactions of atomic oxygen with carbon clusters C_n lead to the production of CO as the preferred channel with rather high rate constants, 10^{-10} cm^3 s^{-1}. The channel leading to "oxygen-carbon chains" C_nO could also be rapid, even with a lower branching ratio. In IRC +10216, various carbon chains such as l-C_3H, C_3N, and C_4H are found to be located in shells with radii near $r \sim 15''$ (Guélin et al. 1993). The abundances of these chains are factors of 10–1000 times larger than that of C_3O [$N_{tot}(C_3H) = 7.0 \times 10^{13}$ cm^{-2}, $N_{tot}(C_3N) = 2.5 \times 10^{14}$ cm^{-2}, $N_{tot}(C_4H) = 3.0 \times 10^{15}$ cm^{-2}; Cernicharo et al. 2000]. Hence, there is a large reservoir of starting material for the formation of C_3O via reactions of carbon chain precursors with atomic oxygen. Although oxygen is primarily locked into CO throughout most of the envelope due to a self shielding effect, ^{13}CO is more readily photodissociated in the inner regions and could be the oxygen donor, as discussed by Agúndez & Cernicharo (2006).

In order to investigate the effect on the C_3O abundance of the oxygen-carbon chain channel, we have run the chemical model including the following two reactions separately:

$$O + C_4 \rightarrow C_3O + C, \qquad k_1 = 7 \times 10^{-12} \text{ cm}^3 \text{ s}^{-1}, \quad (1)$$

$$O + l - C_3H \rightarrow C_3O + H, \qquad k_2 = 2 \times 10^{-10} \text{ cm}^3 \text{ s.}^{-1} \quad (2)$$

Both reactions are exothermic and spin-allowed. The rate constants assumed here are reasonable for these types of reactions, although they were adjusted to produce the observed C_3O line profiles, corresponding roughly to a radial column density of $\sim 10^{12}$ cm^{-2}. The predicted C_3O abundance profiles are plotted in Figure 2, labeled as $C_3O^{[O+C_4]}$ and $C_3O^{[O+C_3H]}$ for the cases when reactions (1) and (2), respectively, are included. The resulting spatial distribution of C_3O predicted by this model is extended ($r = 20''$–$30''$) and the line profiles U-shaped, in agreement with the observations (see Fig. 1, *dashed lines*).

4.3. *Implications for Oxygen Chemistry in Carbon-rich Circumstellar Envelopes*

The probable origin of C_3O in IRC +10216 is in gas-phase reactions in the outer envelope, either ion-molecule or neutral-neutral processes. While it has been suggested that the O-bearing molecules H_2O, OH, and H_2CO in IRC +10216 originate from cometary ices, C_3O is unlikely to have such a source. The composition of comets is thought to reflect pristine interstellar material (Mitchell et al. 1981) and hence common abun-

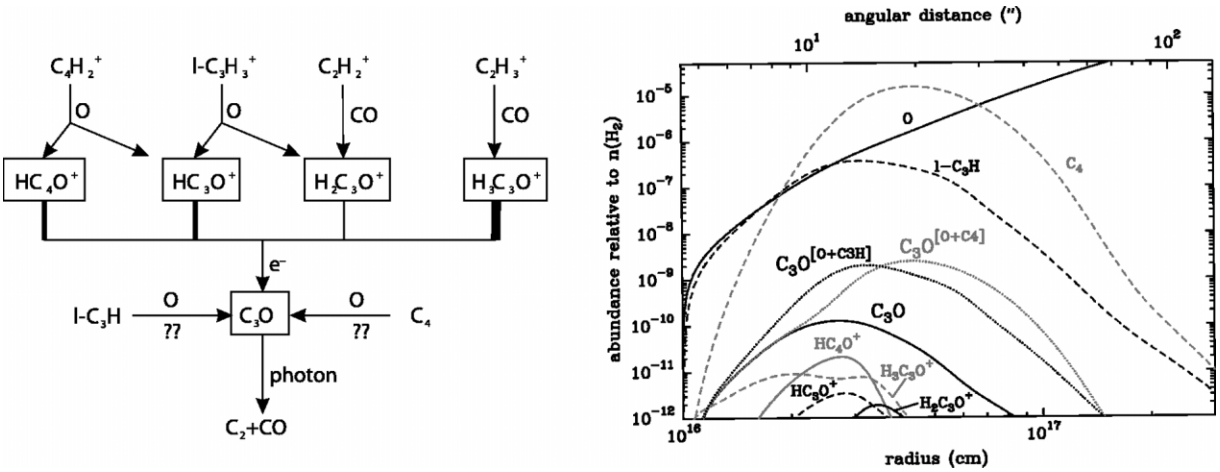

FIG. 2.—Chemical scheme illustrating the main formation routes to C_3O (*left*), and abundance profiles generated by the chemical model for this molecule and related species (*right*). The lines indicated by $C_3O^{[O+C_4]}$ and $C_3O^{[O+C_3H]}$ show the C_3O abundance when reactions (1) and (2) are individually included in the model. Scale for the top axis is angular distance for an assumed stellar distance of 150 pc.

dances in molecular clouds. C_3O has only been observed previously in one other source, the cold, dark cloud TMC-1 (Brown et al. 1985; Kaifu et al. 2004). The environment in TMC-1 is unusually carbon-rich for a dense cloud, as evidenced by the series of acetylenic chains found in this object (Kaifu et al. 2004). Such chains do not appear to be particularly abundant in dense clouds near high-mass star-forming regions, such as Orion KL or Sgr B2(N) (A. J. Apponi et al. 2006, in preparation). Moreover, C_3O has never been observed in a comet.

The detection of C_3O in IRC +10216, combined with our model results, is evidence that gas-phase oxygen-rich chemistry is occurring in the outer shell. Neutral-neutral reactions involving atomic oxygen are an important component of this synthesis and are a viable alternative to the icy-body vaporization theory in explaining the presence of O-bearing molecules in IRC +10216, as suggested by Agúndez & Cernicharo (2006). These authors predict that species such as SO, NO, OCS, and NCO also exist in the outer envelope with nonnegligible abundances, ranging from 10^{-11} to 10^{-9}. Searches for these compounds in IRC +10216, all of them undetected within the sensitivity of the IRAM 30 m 3 mm line survey (J. Cernicharo et al. 2006, in preparation), will be critical tests of this model, and examination of their distributions will help further define the processes leading to oxygen-bearing molecules in carbon-rich circumstellar envelopes.

This material is based on work supported by the National Aeronautics and Space Administration through the NASA Astrobiology Institute under Cooperative Agreement CAN-02-OSS-02 issued through the Office of Space Science. We also acknowledge support from Spanish MEC under project AYA2003-2785 and from "Comunidad de Madrid" under PRICIT project S-0505/ESP-0237 (ASTROCAM). E. D. T. thanks NSF for a graduate research fellowship, and M. A. acknowledges Spanish MEC for a predoctoral grant AP2003-4619.

REFERENCES

Agúndez, M., & Cernicharo, J. 2006, ApJ, in press (astro-ph/0605645)
Brown, R. D., et al. 1985, ApJ, 297, 302
Bujarrabal, V., Fuente, A., & Omont, A. 1994, A&A, 285, 247
Cernicharo, J., Guélin, M., & Kahane, C. 2000, A&AS, 142, 181
Fong, D., Meixner, M., & Shah, R. Y. 2003, ApJ, 582, L39
Ford, K. E. S., Neufeld, D. A., Goldsmith, P. F., & Melnick, G. J. 2003, ApJ, 589, 430
Ford, K. E. S., Neufeld, D. A., Schilke, P., & Melnick, G. J. 2004, ApJ, 614, 990
Green, S., & Chapman, S. 1978, ApJS, 37, 169
Guélin, M., Lucas, R., & Cernicharo, J. 1993, A&A, 280, L19
Hasegawa, T. I., et al. 2006, ApJ, 637, 791
Herbst, E., Smith, D., & Adams, N. G. 1984, A&A, 138, L13
Kaifu, N., et al. 2004, PASJ, 56, 69
Melnick, G. J., Neufeld, D. A., Ford, K. E. S., Hollenbach, D. J., & Ashby, M. L. N. 2001, Nature, 412, 160
Milam, S. N., Ziurys, L. M., Apponi, A. J., & Woolf, N. J. 2006, Nature, submitted
Millar, T. J., Herbst, E., & Bettens, R. P. A. 2000, MNRAS, 316, 195
Mitchell, G. F., Prasad, S. S., & Huntress, W. T. 1981, ApJ, 244, 1087
Morris, M., Gilmore, W., Palmer, P., Turner, B. E., & Zuckerman, B. 1975, ApJ, 199, L47
Savage, B. D., & Sembach, K. R. 1996, ARA&A, 34, 279
Smith, I. W. M., Herbst, E., & Chang, Q. 2004, MNRAS, 350, 323